Electronic Supplementary Material (ESI) for ChemComm.

Supplementary information:
Two Solvent Grinding Sonication Method for the Synthesis of Two-dimensional Tungsten Disulphide Flakes

Benjamin J. Carey[a,b], Torben Daeneke[a], Emily P. Nguyen[a,b], Yichao Wang[a], Jian Z. Ou[a], Serge Zhuiykov[b] and Kourosh Kalantar-zadeh[a]

[a] School of Electrical and Computer Engineering, RMIT University, Melbourne, Victoria, Australia

[b] Division of Materials Science and Engineering, CSIRO, Highett, Victoria, Australia

Experimental Methods

Materials

Tungsten disulphide (WS_2) 2 µm powder (CAS Number 12138-09-9) was purchased from Sigma-Aldrich®. N-methyl-1-pyrrolidine (NMP), acetonitrile (ACN) and absolute ethanol were purchased from commercial chemical suppliers and were not purified or treated in any way and the water used was Milli-Q filtered water (>18 MΩ).

Synthesis of Two-dimensional WS_2 flakes

For each of the four batches 1 g of WS_2 was ground with a mortar and pestle for 30 minutes with 1 ml of solvent added periodically for a total of 5 ml/g. in the case of the single solvent method additional solvent was added to form 15 ml of slurry. For the two solvent method, the grinding solvent was left to dry for 1 hour at room temperature before the second solvent was added to form 15 ml of slurry. The solutions were then probe sonicated at 100 W for 90 minutes in an ice bath to prevent excessive heating. The solutions were then centrifuged at 2500 RPM for 45 minutes and the supernatant was collected.

Measurement and Characterization

Transmission electron microscope imaging was performed with a JEOL 1010 TEM operating at 100 kV, and JEOL 2100F scanning transmission electron microscope (STEM) operating at 80 kV both fitted with SC600 CCD Cameras (Gatan Orius), 10-100 µl dripped onto a 300 mesh copper holey carbon grid (ProSciTech, Australia).

Atomic force microscopy imaging was performed using a Phillips D3100 scanning probe microscope (AFM/SPM) in tapping mode, 5 µL of solution was drop-casted onto a standard silicon substrate. Conductive AFM images were obtained using a Bruker

MultiMode with an installed Peak Force TUNA module (MM8-PFTUNA for MultiMode8 AFM system).

UV-Vis absorption was measured using a Cary 60 spectrometer (Algilent Technologies) with baseline correction in a standard UV glass cuvette. Samples were diluted 1:4 in the case of NMP and the two-solvent method exfoliated flakes.

Raman spectroscopy was carried out using a Renishaw inVia confocal microscope system. Specimens were illuminated with an argon laser (514 nm wavelength) through a 50× objective, laser was approximately 7 mW and the spot size in the range of 1 μm. 20 μL of solution was drop-casted onto a gold coated (200 nm) silicon substrate.

X-ray diffraction (XRD) patterns were obtained using RMIT Bruker D4 Endeavour wide-angle diffractometric with a (Cu K-alpha) 0.15418 nm X-ray source. Dynamic-Light scattering (DLS) particle sizing was completed using an ALV Fast DLS particle sizing spectrometer. Thermo-gravimetric analysis (TGA) was carried out using a Perkin Elmer, Pyris1 TGA from 50°C-800°C under nitrogen gas flow and then from 800-850°C in air. 5 mg of dried WS_2 flakes were used, the NMP exfoliated flakes were dried in a vacuum oven (~500 mmHg) at 70°C for 100 hours. In the case of the two solvent exfoliated flakes the sample was dried at 70°C for 5 hours under a stream of nitrogen. Prior to the actual TGA measurement the sample was kept at 70°C for 30 minutes while recording the weight loss. No weight loss was observed indicating that a stable state had been reached and the sample was dry.

Hansen Solubility Parameters

The HSP distances R_a were calculated using:

$$R_a = \left[4\left(\delta_{D,solvent} - \delta_{D,solute}\right)^2 + \left(\delta_{P,solvent} - \delta_{P,solute}\right)^2 + \left(\delta_{H,solvent} - \delta_{H,solute}\right)^2\right]^{0.5}$$

where δ_D, δ_P, and δ_H are the dispersive, polar, and hydrogen-bonding solubility parameters of the solvent and solute, respectively. [1]

In the case of mixed solvent the HSP values can be calculated as a linear function of composition thus for the 50/50 ethanol/water mixtures the each effective HSP (D, P and H) value is simply the mean of ethanol and water.[1]

The HSP values for WS_2 and the solvents were obtained from Coleman *et al.* and Hansen Solubility Parameters, A User's Handbook, 2nd Ed respectively.[2, 3]

Solution Concentrations

The concentrations of the solutions were calculated using the UV-Vis absorption data and the methodology outlined by O'Neill et al.[4], whereas the resonant absorbance per unit length [$^{(A/l)_r}$] is directly related to the concentration independent of scattering effects:

$(A/l)_r = \alpha_r C$

where α_r is the resonant absorption coefficient. [4] The value of α_r for WS_2 was obtained from Coleman et al.'s work.[2] This method yields concentrations of 0.14 mg/ml, 1.46 µg/ml, 0.82 µg/ml and 0.1 mg/ml for NMP, ACN, ethanol/water and the two solvent method respectively.

Experimental Section

Reverse Two-solvent Method

The order for the implementation of the two-solvent solution was reversed (grinding in ethanol/water, sonication in ACN) and the exfoliation process was repeated. This experiment was attempted as a control test. The procedure was accomplished using an almost identical method to the ACN grinding, ethanol/water sonication solution with the exception of an increase in post-grinding drying time (which was necessary due to the higher boiling point of water). In the case of the reverse method the WS_2 ethanol/water slurry was left to dry overnight (at room temperature).

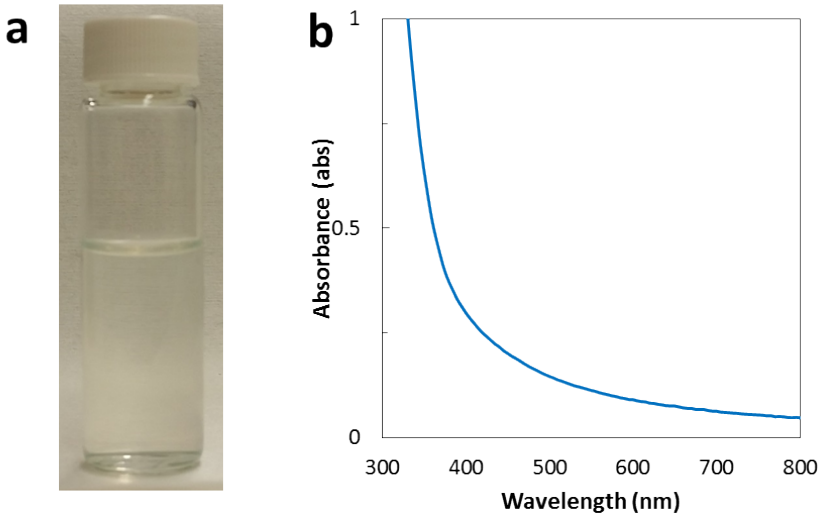

Figure S1: (a) Photograph and (b) UV-Vis absorption spectra of WS_2 suspension after the process involved grinding in ethanol/water (50/50) and sonication in ACN.

The reverse two solvent method was however unable to effectively increase the yield. As can be seen in figure S1, the reverse two-solvent method produced low optical contrast and very little UV-Vis absorbance characteristics analogous to the results produced by both ACN and ethanol/water single solvent methods. In fact the concentration of the reverse method was calculated (see above for method) to be reduced to 0.77 µg/ml, less than both of the formers.

Sample AFM Images

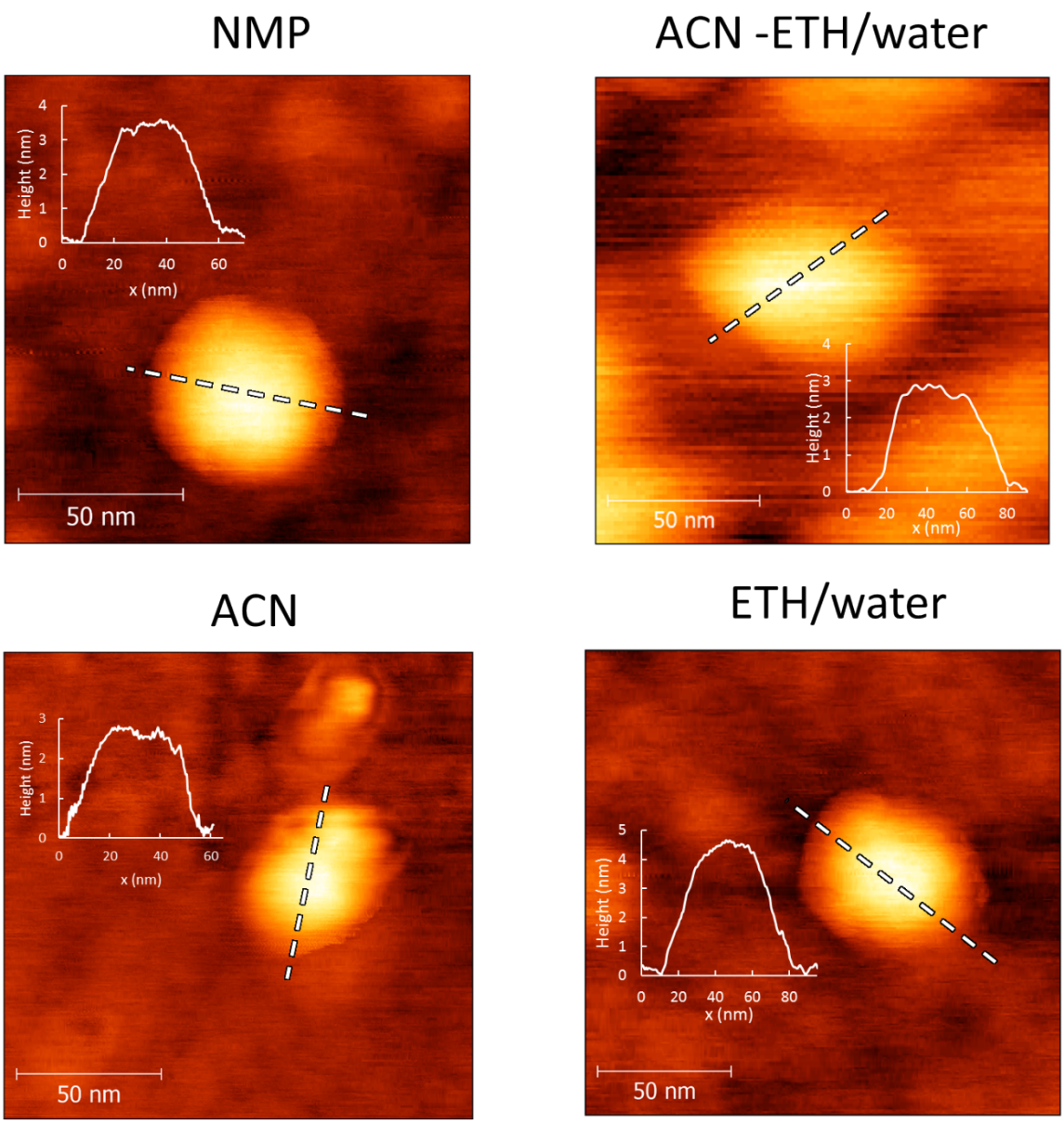

Figure S2: Sample AFM images of the exfoliated WS_2 flakes deposited on Si substrates.

Typical AFM images of the WS_2 solutions are displayed in figure S2. The statistical analysis presented in figure 2 (a-d) were assessed from AFM images such as (and including) these by assessing the height of approximately 100 flakes. Similarly both the AFM and TEM images such as (and including) those presented in figure 2 (i-l) were used for statistical analysis of the lateral dimensions.

Conductive AFM Analysis

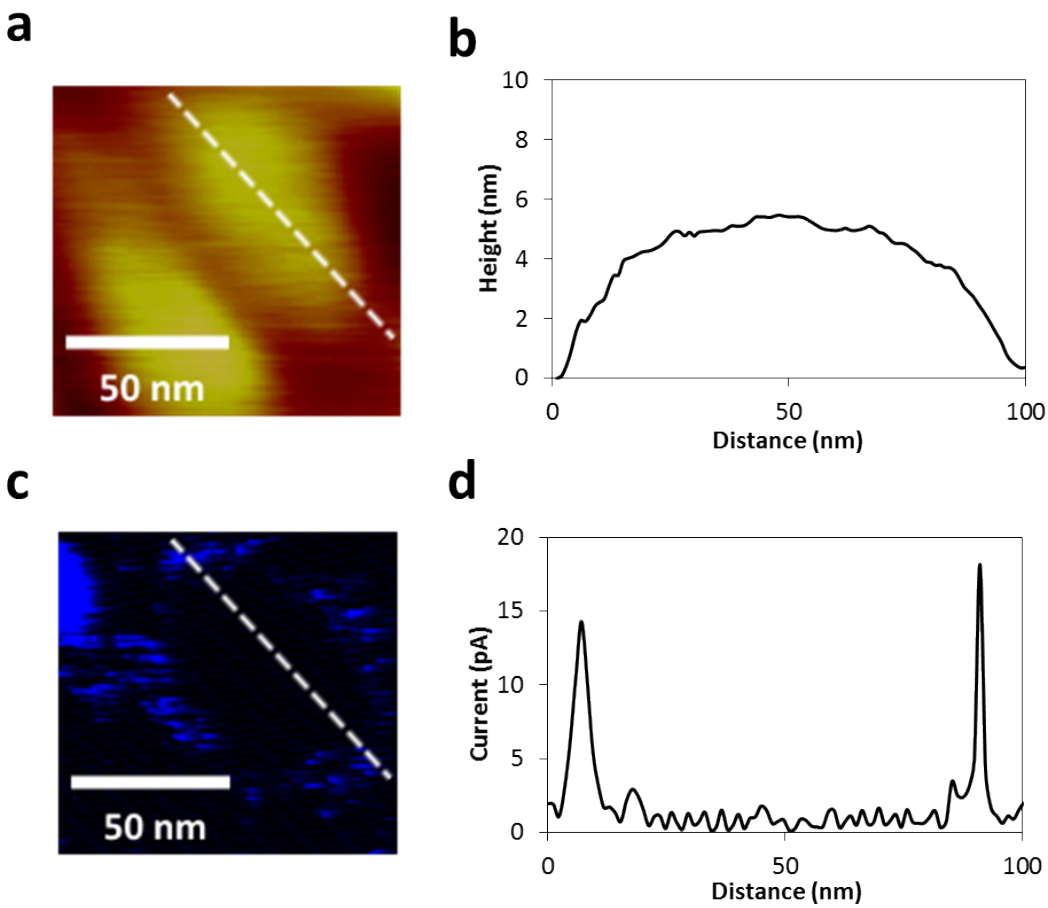

Figure S3: Conductive Atomic Force Micrograph of WS_2 flakes exfoliated via the two solvent method on Au substrate representing both (a) height and (c) tip current of the same area. B and D are the profiles the white dashed line in A and B respectively.

It has been shown that liquid exfoliated transition metal dichalcogonides (TMDs) can contain defects in the crystal structure, resulting in metallic edges.[5] Conductive AFM (figure S3) has been used for elucidating this effect. With the profiles in figure S3 it is apparent that the edges of most of the WS_2 flakes are conductive.

Raman Spectroscopy

Table S1: Summary of Raman shift peak intensities and locations for the $2LA(M)$, $E_{2g}^{1}(\Gamma)$ and $A_{1g}(\Gamma)$ phonons (intensities are normalized to the $A_{1g}(\Gamma)$ peak).

	$2LA(M)$		$E_{2g}^{1}(\Gamma)$		$A_{1g}(\Gamma)$	
	Intensity	Peak shift (cm^{-1})	Intensity	Peak shift (cm^{-1})	Intensity	Peak shift (cm^{-1})
Bulk	0.52	350.6	0.22	356.0	1	420.4
NMP	0.42	352.5	0.28	357.7	1	422.5
ACN	0.41	354.2	0.36	358.2	1	425.5
Ethanol/water	0.41	352.8	0.48	359.8	1	428.0
ACN-ethanol/water	0.48	353.0	0.51	358.9	1	425.2

The information of phonon peak intensities and positions are recorded in Table S2. Here it is clear that the 2D and quasi-2D WS_2 flakes produce a comparative increase in the $E_{2g}^{1}(\Gamma)$ phonon peak which is a phonon in the horizontal plane as opposed to the $2LA(M)$ and $A_{1g}(\Gamma)$ phonon peaks that are vertical plane phonons and thus relay upon interlayer interactions.[6]

HRTEM

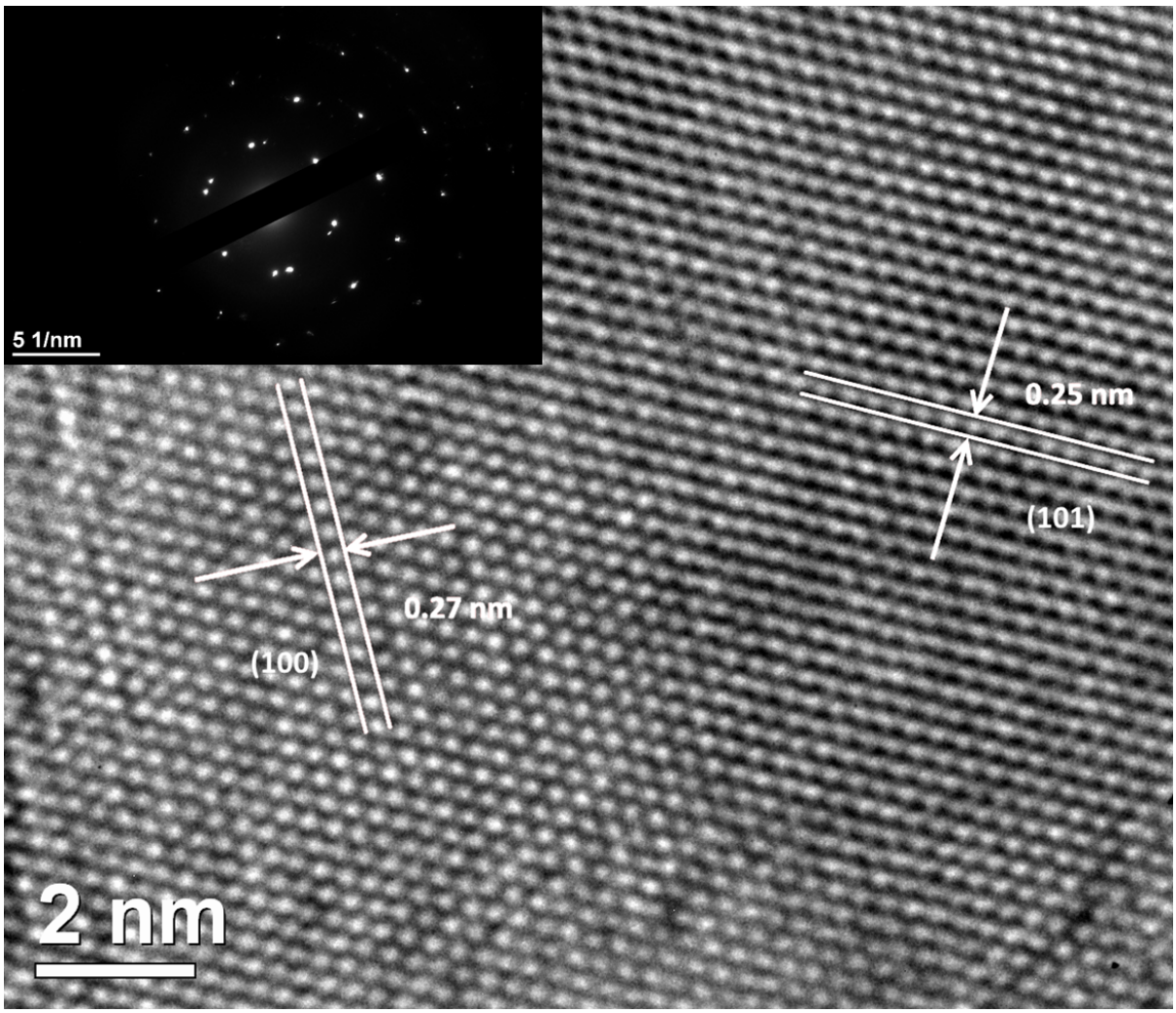

Figure S2: High resolution transmission electron micrograph (HRTEM) of the exfoliated WS_2. Insert is a selected area electron diffraction (SAED) image of the same section.

Figure S2 displays a HRTEM image of the 2D WS_2 here both the 1.0.0 and 1.0.1 crystal planes are visible in two distinct crystal domains. These lattice spacing correlate with the XRD pattern in Figure 3 at 32.7° and 33.5°.

Analysis of XRD Results

Table S2: Summary of vertical plane XRD results for the comparison of the crystallographic effects of grinding WS_2 with different solvents.

Paracrystallinity (%)				
Crystal plane	Bulk	NMP	ACN	Ethanol/water
002	0.793	0.730	0.979	0.847
004	1.244	1.128	1.347	1.075
006	1.266	1.259	1.264	1.265
008	0.754	0.545	0.766	0.642
Normalized Peak Intensity				
Crystal plane	Bulk	NMP	ACN	Ethanol/water
002	1	1	1	1
004	0.082	0.102	0.072	0.083
006	0.083	0.102	0.065	0.075
008	0.023	0.004	0.022	0.009
Normalized Integral Intensity				
Crystal Plane	Bulk	NMP	ACN	Ethanol/water
002	1	1	1	1
004	0.117	0.139	0.102	0.104
006	0.143	0.150	0.110	0.112
008	0.115	0.022	0.080	0.041
Full-width half-maximum (FWHM) (2θ °)				
Crystal plane	Bulk	NMP	ACN	Ethanol/water
002	0.085	0.105	0.130	0.105
004	0.125	0.140	0.165	0.140
006	0.095	0.180	0.219	0.185
008	0.569	1.517	0.888	0.818

The paracrystallinity of the WS_2 was calculated as

$$g = \sqrt{\frac{\langle d^2 \rangle - \langle d \rangle^2}{\langle d \rangle^2}}$$

where g is the paracrystalline factor, and d is the planar spacing.[7]

References

1. K.-G. Zhou, N.-N. Mao, H.-X. Wang, Y. Peng and H.-L. Zhang, *Angewandte Chemie-International Edition*, 2011, **50**, 10839-10842.
2. J. N. Coleman, M. Lotya, A. O'Neill, S. D. Bergin, P. J. King, U. Khan, K. Young, A. Gaucher, S. De, R. J. Smith, I. V. Shvets, S. K. Arora, G. Stanton, H.-Y. Kim, K. Lee, G. T. Kim, G. S. Duesberg, T. Hallam, J. J. Boland, J. J. Wang, J. F. Donegan, J. C. Grunlan, G. Moriarty, A. Shmeliov, R. J. Nicholls, J. M. Perkins, E. M. Grieveson, K. Theuwissen, D. W. McComb, P. D. Nellist and V. Nicolosi, *Science*, 2011, **331**, 568-571.
3. C. M. Hansen, *Hansen solubility parameters: a user's handbook*, CRC press, 2012.
4. A. O'Neill, U. Khan and J. N. Coleman, *Chemistry of Materials*, 2012, **24**, 2414-2421.
5. C. Backes, R. J. Smith, N. McEvoy, N. C. Berner, D. McCloskey, H. C. Nerl, A. O'Neill, P. J. King, T. Higgins, D. Hanlon, N. Scheuschner, J. Maultzsch, L. Houben, G. S. Duesberg, J. F. Donegan, V. Nicolosi and J. N. Coleman, *Nature Communications*, 2014, **5**, 4576.
6. A. Berkdemir, H. R. Gutierrez, A. R. Botello-Mendez, N. Perea-Lopez, A. L. Elias, C.-I. Chia, B. Wang, V. H. Crespi, F. Lopez-Urias, J.-C. Charlier, H. Terrones and M. Terrones, *Scientific Reports*, 2013, **3**, 1755.
7. D. Palit, S. K. Srivastava, M. C. Chakravorti and B. K. Samantaray, *Journal of Materials Science Letters*, 1996, **15**, 1636-1637.